Correspondence of Alkalinity and Ferric/Ferrous Ratios of Igneous Rocks Associated with Various Types of Porphyry Copper Deposits

JAN C. WILT *Woodward-Clyde Federal Services, Las Vegas, Nevada*

ABSTRACT

The magma metal series classification of ore deposits developed by S. Keith of MagmaChem Exploration, Inc., and neural networks, a new type of pattern recognition software, have profound implications to metallogenesis and have promising applications to mineral exploration and to alteration and zoning studies. These techniques were evaluated by assigning 43 deposits to six subclasses of the magma metal series classification defined on eight variation diagrams, training neural networks to classify analyses of 205 igneous and 887 mineralized samples, and testing the networks on their ability to classify new data.

Porphyry copper deposits are characteristic of six different alkalinity and ferric/ferrous ratio categories in the magma metal series classification. Such deposits occur in calcic weakly oxidized, calc-alkalic oxidized, calc-alkalic weakly oxidized, quartz alkalic oxidized, quartz alkalic weakly oxidized, and nepheline alkalic oxidized subclasses. The calc-alkalic oxidized subclass includes world class porphyry copper deposits with the best grade and tonnage characteristics.

Only two of the foregoing six subclasses were studied in detail; these were compared to four other deposit types of different alkalinity and oxidation character. Whole rock oxides of fresh igneous rocks were correlated with trace elements in rock chip samples from temporally and spatially associated ore deposits of the six alkalinity and oxidation subclasses. The K_2O versus SiO_2 diagram best defined the alkalinity classes of calc-alkalic and alkali-calcic; SiO_2/K_2O ratios of alkali-calcic igneous rocks range between 14 and 20, and those of calc-alkalic rocks are between 20 and 30. Iron mineralogy and the Fe_2O_3/FeO versus SiO_2 diagram best defined oxidation subclasses of oxidized, weakly oxidized, and reduced; Fe_2O_3/FeO ratios are more than 0.8 and magnetite and sphene are abundant for oxidized subclasses, between 0.5 and 1.2 with magnetite, sphene, and rare ilmenite for weakly oxidized subclasses, and less than 0.6 with only ilmenite for reduced subclasses.

Whole rock analyses from fresh igneous rocks were obtained from mining districts for which trace element geochemistry was also available. Lead-zinc-silver deposits such as Tombstone, Tintic, and Park City are related to oxidized alkali-calcic igneous rocks. Polymetallic lead-zinc-copper-tin-silver deposits such as Santa Eulalia, Railroad, Taylor, and Tempiute are associated with weakly oxidized alkali-calcic igneous rocks. Tin-silver deposits of Llallagua and Potosi are correlated with reduced alkali-calcic intrusives. Porphyry copper deposits such as Ray, Christmas, Mineral Park, Highland Valley Copper, and Sierrita are derived from oxidized calc-alkalic plutons. Gold-rich porphyry copper deposits such as Copper Canyon, Ajo, El Salvador, El Teniente, Hedley, and Morenci are linked to weakly oxidized calc-alkalic plutons. Disseminated gold deposits such as Chimney Creek, Getchell, Carlin, and Northumberland are temporally and geochemically correlated with reduced calc-alkalic igneous rocks, but physical connections between plutons and Carlin-type deposits are rarely obvious.

Learning vector quantization and back-propagation artificial neural networks correctly classified 100 percent of igneous samples and 99 percent of mineralized samples. Discriminant analysis correctly classified only 96 and 83 percent of such samples respectively. Neural networks trained with 90, 80, 70, or 50 percent of the samples correctly classified 81 to 100 percent of the randomly withheld samples. The high degree of correspondence between chemistries of igneous rocks and related mineralization implies genetic links between magmatic processes or sources and the ore deposits studied.

INTRODUCTION

The magma metal series classification developed and used in the exploration industry by Stanley Keith (Keith and others, 1991) predicts that certain types of ore deposits are associated with particular categories of aluminum content, alkalinity, and oxidation character in fresh igneous rocks that are spatially and temporally related to mineralization. The classification contains 75 subclasses, many of which are not well represented by analyses in the geologic literature (table 1). Only six of the best documented subclasses were selected for study here.

THEORETICAL BASIS OF MAGMA METAL SERIES CLASSIFICATION

The magma metal series classification is based on the concept that a suite of comagmatic igneous rocks evolves along a differentiation path and produces a hydrothermal ore deposit as the final, fluid-rich phase in the crystallization sequence (Keith and others, 1991). This concept predicts a consistent chemical link between parent magma and daughter mineral deposit; if metals in a hydrothermal ore deposit are the extremely differentiated residue of a parent magma, then exploration predictability is intrinsic to the magma series classification.

The empirically derived magma metal series classification of a deposit is based on the alkalinity, oxidation character, and aluminum/alkali ratio of igneous rocks that are temporally and spatially associated with the deposit. Alkalinity is based on Peacock's (1931) alkali-lime index classes of plutonic rocks (fig. 1). Further subdivisions of the alkalinity classification are based on oxidation character as measured by ferric/ferrous (Fe_2O_3/FeO) ratio and on the presence and variety of accessory minerals, such as the magnetite/ilmenite distinction of Ishihara (1977, 1981). The aluminum/alkali ratio defines the broader distinction between peraluminous and metaluminous categories

Alu	Alkalinity	Oxidatio	metal production	important trace elements
Per	Calcic	r	Au	As, U, Th
		o	Au-Ag	As, Pb, Zn, Cu, U, Th, V
		ow	Au-Ag	Pb, Zn, Cu
	Calc-alkalic	r	W-Pb-Zn-Ag	Be, F, Sn, Li, Ta, P
		o	W-Be-Pb-Zn-Ag	F, Bi, B
	Alkali-calcic	r	Sn-W-Cu-U-Pb-Zn-Ag-Li-C	As, F, B, Rb, Nb, Bi, Te, P
		o	U-W	
	Alkalic	r to o	U-Th	Co, Ni, As, Bi
Met	Magnesian	very r	Au>>Ag	As, Co, Ni, Cr
		r	Ni>>Cu, Pd, Co	As
		ow	Cr (ios); Cu>Zn-Au-Ag	Co, Ni, Mn, Fe
	Calcic	very r	Au>Ag	As, CO2, Co, Ni, B, Li
		r	Au>Ag	As, Cu, Bi, Pb, Zn
		ow	Cu>Zn-Au-Ag; Cu-Zn-Ag>Au	Mo, Co; Bi, F, As, Pb
		very r	PGE-Au	Bi-Te-FeO-As-low S
		r	Cu-Co-Ni-PGE; Zn>Cu-Ag-Au ■	As, FeO, high S; Co-As, Mn, Fe
	Calc-alkalic	very r	Au>Ag	As, CO2, B, Sb, Hg, W
		r	Au>Ag ●	As,Sb,Hg,Tl,W,LREE,Zn,Cu,V,Ni,Ba,low S
		ow	Cu-Au-Ag-Zn-Mo-Pb ■ ●	Bi-As-Sb-V-Sc-P
		o	Cu-Zn-Pb-Ag>>Au-Mo-Mn ■ ●	As, B, W
		mod o	Cu; W-Cu-Mo; S; Pb-Zn-Ag-Au-Ba	As-Te-Bi-Se-Sn; Ag>>Ag, Bi,Pb,Zn; Bi-Sb-Hg-Tl-As
		os	Mg	W-Cu
		very r	Au	PGE, low S, FeO, As
		r to ow	Zn>C_{α}Pb-Ag	Ba
		r	none known	
		very r to r	none known	
	Alkali-calcic	ow to o	none known	
		rs to r	Ag	Co, Ni, As, Bi, U
		r to ow	Sn-Ag ●	Zn, Cu, In, Ga, As, B, Y, F, P
		ow to o	Pb-Zn-Ag; Ag>>Au ●	Sn,Bi,Mn,B,Sb,Hg,As; Pb-Zn-Be, As,Sb,Hg,Bi,Se,F
		mod o	Zn>Pb-Ag-Mn; Ag>>Au, Mn ●	B,Bi,Ba,Sb,Hg,As,Be,Te; Pb-Zn-Be,Ba,Hg,Sb,Bi,Te,
		os	?U-Th; Fe; Mn	Ag,Co,Pb,Bi,Be,F; P,Pb,Zn,Ag,F,V,Y; Be,W,Pb,Zn,Ag,B
		r to ow		
		ow to o	Mo, F	Ag, Pb, Zn, Bi, Sb
		os	U, Th	
		r	Sn	F, Rb
		ow	Mo-Sn	Mn, F, Ga, In, Bi, Rb, W
		o	Mo	Be, Sn, Ga, Pb, Zn, Ag, Bi, F, Mn, Rb, W
		os	Be; Be-F-U	F, Fe, Sn, Mn, W; Mn
		r to ow	none known	
		r to ow	HREE, Y, Hg	LREE, Zr, Mo, Sn, F, Cl, Li, U, Th, Cl
		ow ot o	Nb, Zr, U, Th, F	
		o to os	LREE, Be, Y, U, Th, Zr, Mo, Sn, F	
		r to ow	none known	
		r to ow	Ti-Fe-V	P
	Quartz Alkalic	ow to o	none known	
		r	PGE	Au, Cu, Ni, Co
		ow	Cu-Au<Ag-Pb-Zn; Au>Ag ■	Te, F; Be, F, Mn
		o	Cu-Au-Fe-U-LREE ■	
		os	Fe; U-F; Cu-Ag>>Au-Pg-Zn-U-Mn; Cu,Ag,Au	P,F,V,Y,Sc; Mo; Bi; Fe; Be,W,Fe
		ow to om	Cu-Au<Ag, PGE,PB,Zn,Mo; PGE■	Te, F, Mn, Co, Ni; Au, Ni, Cr, Co, As, Fe
		r to ow	none known	
		ow to o	Nb-Zr-U-Th-Be	F, LREE, Y
		r to ow	Ti-Fe-V	P
	Nepheline Alkalic	ow to o	none known	
		r	Au>Ag	Te, Fe, Co, Mo, Ba, Sr, Rb
		ow to o	Cu-Au ■	Mo
		os	U, Th	LREE, Pb>Zr, Ag>Ar, LREE, Ba, Sr
		r to ow	none known	
		r to ow	Hg	F, Li, U, Zr, Cl
		ow to o	Al	Zr, Y, Ti, F, Cl
		o to os	LREE, Zr, U, Th, Y	Mo, Nb, F, Cl
	Hyperalkalic	r to ow	none known	
		ow to o	none known	
		r to ow	Nb?	
		ow to os	Cu, Fe, Au, P, U, Th, Zr, Sr, Ba	LREE, Nb, Ta
		os	LREE	Ba-Sr-Cu
		r to ow	Ti>Nb, Fe	P, Pb, Zn, Ag, Ba, Zr
		o	Nb>>Ti, P, Fe, Mn	LREE, Zr
		o	Cu, Au	Ba, Sr, Ag
		r to ow	none known	
		ow	none known	
	Ultra-alkalic	r	C	diamonds
	kimberlite-lam	o	none known	
	HighK Ultra-alk	o to os	none known	

Table 1. Magma metal series classification showing logical subdivisions of aluminum content, alkalinity, oxidation state, and selected metal specializations (from Keith and others, 1991).

based on the A/CNK index of Shand (1927), which is molecular $Al_2O_3/(CaO+Na_2O+K_2O)$. Boundaries between classes have been drawn between clusters of each ore deposit type on variation diagrams. If the empirical derivation of the classification reflects a natural distinction, then the magma metal series class of an igneous rock will predict the type of ore deposit associated with that rock.

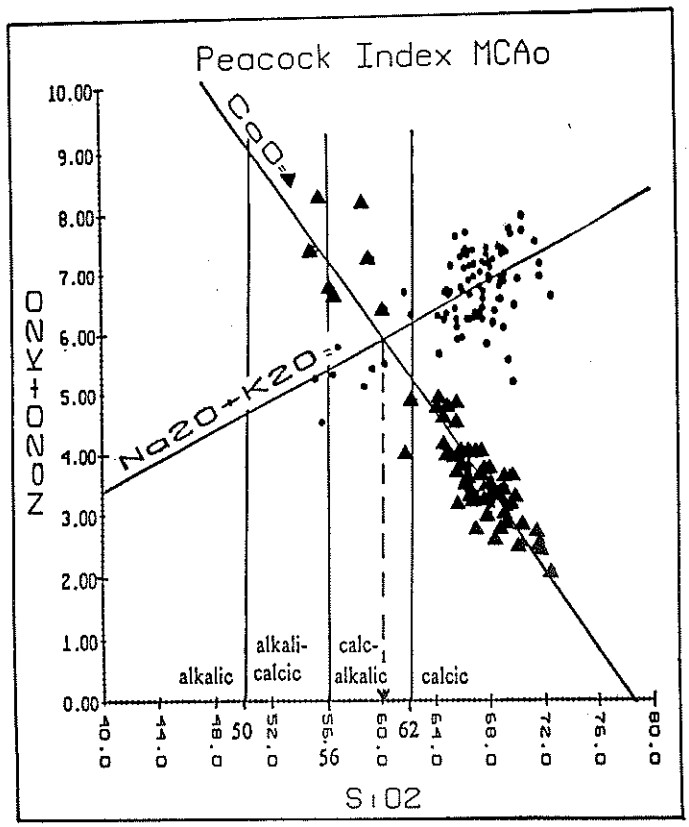

Figure 1. Variation diagram illustrating the technique used by Peacock (1931) to determine the alkali-lime index, often called the Peacock index.

Aluminum Content and Alkalinity (Source Region)

The hierarchy of subclasses from highest to lowest orders is based on aluminum content, alkalinity, water content, iron content, halogen content, and oxidation character (Keith and others, 1991). The first distinction of aluminum content is between peraluminous (A/CNK index more than 1.0) or metaluminous (A/CNK index less than 1.10). These classes are then subdivided according to alkalinity into magnesian, calcic, calc-alkalic, alkali-calcic, and alkalic subclasses according to fields on Harker variation diagrams such as K_2O versus SiO_2 (fig. 2a), K_2O – CaO versus SiO_2 (fig. 2b), and K_2O – MgO versus SiO_2 (fig. 2c). Hydrous and anhydrous subdivisions are based on water content as shown by other diagrams and the presence of hydroxyl-bearing minerals. Additional categories are based on iron content; these classes are shown on a modified Miyashiro diagram (fig. 2d) in which FeO^*/MgO is plotted against SiO_2 where FeO^* is $0.9(Fe_2O_3)$ + FeO. Further subclasses are based on oxidation character and on halogen content; oxidation subclasses include strongly reduced, reduced, weakly oxidized, oxidized, moderately oxidized, and strongly oxidized, as shown on diagrams of ferric/ferrous ratio (Fe_2O_3/FeO) versus SiO_2 (fig. 2e).

Source and original composition of magma affect aluminum content and alkalinity. Melting and other processes within the crust affect iron, water, and volatile contents, oxidation character, and degree of differentiation. Melting in different layers in the source region of the mantle results in different original compositions. Iron, water, and volatile contents and the oxidation-state conditions that a magma encounters as it ascends affect the sequential crystallization process of Bowen's reaction series because different minerals are stable under different conditions. Which volatiles are present in the lower or middle crust is extremely important in determining the final metal content of an ore deposit because the oxidation state of the crust influences which minerals crystallize first. The ability of the earlier-formed minerals to accommodate certain metals in their structure determines which metals are concentrated in the hydrothermal fluid and therefore in the ore deposit. This crustal influence is superimposed on fundamentally different magma types determined by depth of magma generation; crustal processes are secondary, whereas magma type or source region is primary.

Iron Content (Crustal Influence)

Metaluminous magmas that are hydrous and of subduction origin are chemically distinguished by magnesium enrichment on a modified Miyashiro plot. Magnesium enrichment results from continuous removal of iron during crystallization of hydrous ferromagnesian minerals such as early hornblende and late biotite. Magnesium enrichment in these magmas is also promoted by the relative lack of minerals such as clinopyroxene that would have preferentially removed magnesium (Keith and others, 1991).

The oxidized/reduced distinction is similar to the magnetite/ilmenite series distinction of Ishihara (1977, 1981) and Takahasi and others (1980). Classification criteria include Fe_2O_3/FeO ratios; mineralogy of accessory sulfides and opaque oxides; magnetic susceptibility; and volume percent and mineralogy of opaque sulfides, oxides, and other accessory minerals such as sphene (Keith and others, 1991).

Oxidation character in the magma metal series classification is determined from mineralogy and from the Fe_2O_3/FeO versus SiO_2 variation diagram. Categories on this diagram include strongly oxidized, moderately oxidized, weakly oxidized, weakly reduced, and strongly reduced subclasses. The reduced or ilmenite-only subclass is characterized by Fe_2O_3/FeO ratios of less than 0.6, the weakly oxidized or ilmenite plus magnetite subclass has Fe_2O_3/FeO ratios between 0.4 and 0.9, and the oxidized or magnetite-sphene subclass has Fe_2O_3/FeO ratios greater than 0.9. Certain indicator minerals in associated mineral deposits have been correlated with the various oxidation subclasses (Keith and others, 1991).

Although oxidation character depends partly on oxygen content of the source region, it mainly reflects modification of magma after its generation. Factors affecting oxidation state of a magma include the amount of water added, the type of crust the magma interacts with, the degree to which the magma differentiates, and the degree to which the magma interacts with atmospheric oxygen in shallow subaerial volcanic environments.

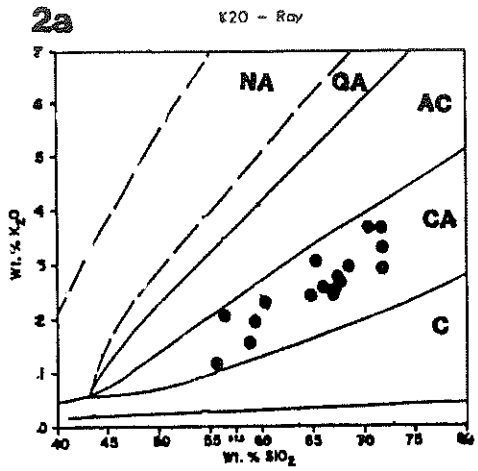

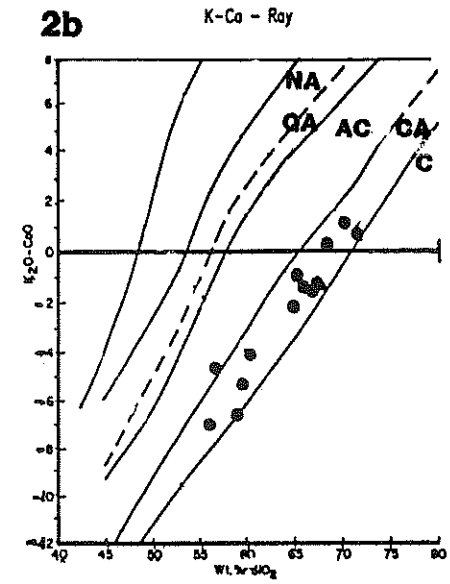

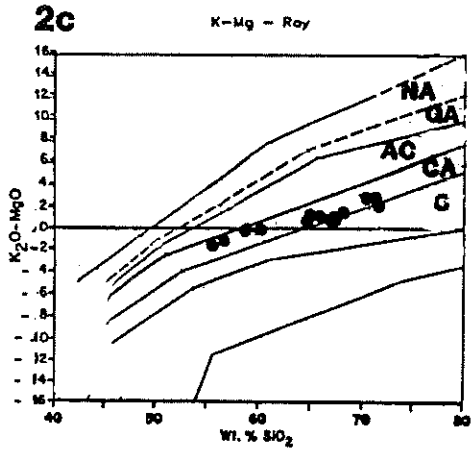

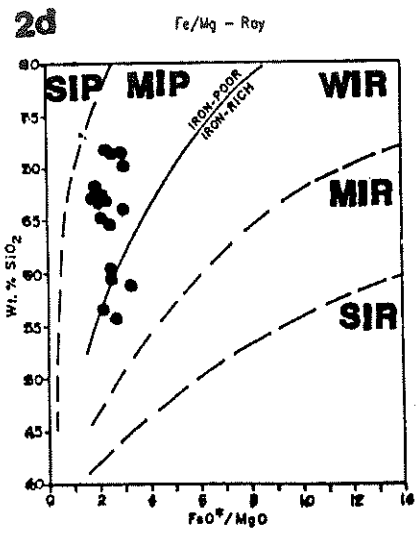

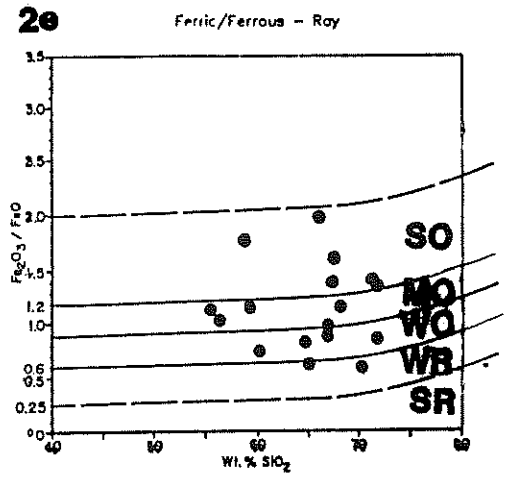

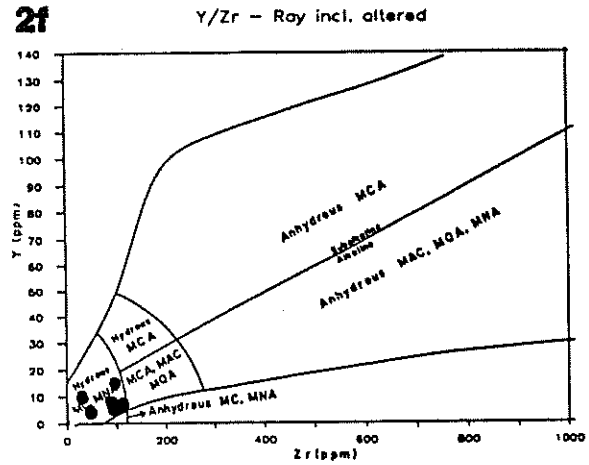

Figure 2. Magma metal series variation diagrams of igneous rocks of the Ray Mining District, Arizona. C is calcic, CA is calc-alkalic, AC is alkali-calcic, QA is quartz alkalic, NA is nepheline alkalic. *2a*. Weight percent K_2O versus weight percent SiO_2. *2b*. Weight percent K_2O minus weight percent CaO versus weight percent SiO_2. *2c*. Weight percent K_2O minus weight percent MgO versus weight percent SiO_2. *2d*. Modified Miyashiro (1974) diagram illustrating iron enrichment; variation diagram plots weight percent SiO_2 versus FeO'/MgO where FeO' is $0.9(Fe_2O_3) + FeO$. SIP is strongly iron-poor, MIP is moderately iron-poor, WIR is weakly iron rich, MIR is moderately iron rich, and SIR is strongly iron rich. *2e*. Ferric/ferrous variation diagram where weight percent Fe_2O_3 divided by weight percent FeO is plotted against weight percent SiO_2. SO is strongly oxidized, MO is moderately oxidized, WO is weakly oxidized, WR is weakly reduced, and SR is strongly reduced. 2f. Y-Zr variation diagram in ppm.

Correlation between oxidation character of plutons and lithotectonic terranes indicates that type of crust has a very important influence on magmatism and associated mineralization. Mid-crustal fluids alter the original oxidation state of magmatic materials from the mantle (Keith, 1991). If the magma is originally reduced and travels through reduced crust, it remains reduced and produces precious metal deposits; if the magma is originally reduced and travels through oxidized crust, it becomes oxidized and produces base metal deposits. Keith asserts that these changes are accomplished by incorporation of mid-crustal formational fluids into the parent magma rather than by melting and assimilating the crust or by mixing solid-state materials in the crust. The degree of contamination of a magma by volatiles or deep crustal fluids varies with the mass number of the element, thus varying degrees of crustal mixing are recorded by different elements in the same pluton.

SIX MAGMA METAL SERIES SUBCLASSES OF PORPHYRY COPPER DEPOSITS

Porphyry copper deposits are common in six different alkalinity and ferric/ferrous ratio subclasses in the magma metal series classification as indicated by the solid squares on table 1. Porphyry copper deposits occur in calcic weakly oxidized, calc-alkalic oxidized, calc-alkalic weakly oxidized, quartz alkalic oxidized, quartz alkalic weakly oxidized, and nepheline alkalic oxidized subclasses.

The calcic weakly oxidized subclass generally produces copper-gold stockwork porphyry deposits in or near low-potassium granodioritic epizonal plutons. Examples include Panguna in Bougainville, Yandera, Ertzberg, and Plesyumi.

The calc-alkalic weakly oxidized subclass produces several types of porphyry copper deposits generally associated with mesothermal medium-potassium granodioritic plutons which contain either biotite and hornblende or only biotite. Examples of moderate-sulfur porphyry copper-gold-molybdenum deposits in or near granodioritic plutons include Ajo, El Salvador, Frieda River, and Morenci. High-sulfur gold-skarn deposits include Hedley and McCoy. High-sulfur gold-lead-zinc-silver fringes of gold-copper-zinc porphyry and or skarn deposits are exemplified by Copper Canyon, Nevada. Hypothermal tungsten skarn-copper-molybdenum deposits at the contact of diorite-granodiorite plutons include Elk Mountain and Mill City.

The calc-alkalic oxidized subclass contains world-class porphyry copper deposits with the best grade and tonnage characteristics. These mesothermal high-sulfur porphyry deposits are primarily copper-silver-molybdenum deposits. The central zones of these districts contain porphyry copper-zinc-molybdenum deposits. These central zones are surrounded by zones of copper-zinc mines, which are in turn surrounded by zones of lead-zinc-silver mines. Furthest from the central zones are zones of silver-manganese mines or prospects. Examples from Arizona of mesothermal high-sulfur porphyry copper-silver-molybdenum deposits are Bagdad, Christmas, Miami-Inspiration, Ray, Mineral Park, San Manuel, Sierrita-Esperanza, Silver Bell, and Twin Buttes-Mission. Bethlehem and Valley Copper in British Columbia are Canadian examples. Other examples are Tyrone, Yerington, Escondida, Sar Cheshmah, Cananea, and Chuquicamata.

The quartz alkalic weakly oxidized subclass includes porphyry copper deposits and or skarn deposits with gold, high sulfur, and sometimes platinum group elements. Examples of quartz alkalic weakly oxidized porphyry copper deposits include Bingham, Copper Flat-Hillsboro, Bajo de la Alumbrera, Ok Tedi, Ely, and Ingerbelle.

The quartz alkalic oxidized subclass includes the porphyry copper deposits of Bisbee, Equity Silver in British Columbia, and Cerrillos in northern New Mexico.

The nepheline alkalic weakly oxidized to oxidized subclass includes epigenetic mesothermal base metal veins and stockworks with very minor gold associated with nepheline-monzonite to syenite plutons. Examples include Caribou-Bell and Galore Creek in British Columbia.

PROCEDURES FOR TESTING CALC-ALKALIC AND ALKALI-CALCIC SUBCLASSES

In order to test the magma metal series methodology, mines were classified into subclasses by whole rock oxides of fresh igneous rocks. Mineralized samples from the same districts were then examined to determine if they could be classified into the same distinct subclasses. Two alkalinity classes (calc-alkalic and alkali-calcic) and three subclasses of oxidation character (reduced, weakly oxidized, and oxidized) were examined for a total of six types of ore deposits shown by solid circles on table 1. Only two of the six magma metal series subclasses that commonly contain porphyry copper deposits were included in this study because of the need to evaluate the methodology on clearly distinct types of deposits. Evaluation was accomplished by assigning 43 deposits to subclasses defined on eight variation diagrams, training neural networks to classify analyses of 253 igneous and 887 mineralized samples, testing the networks on their ability to classify new data, and comparing the results with those obtained on the same data by discriminant analysis (Wilt, 1993).

Whole rock analyses were obtained from the literature and from files of MagmaChem Exploration, Inc. The data consisted of analyses of SiO_2, Al_2O_3, TiO_2, Fe_2O_3, FeO, MnO, MgO, CaO, Na_2O, K_2O, P_2O_5, and loss on ignition (LOI). Approximately 400 samples were obtained from 90 mining districts selected for this study. Forty-two of the 90 mining districts had both sufficient numbers of good quality trace element analyses available from mineralized samples and whole rock analyses available from igneous rocks associated with mineralization. These 42 districts were selected for further study.

Mining districts were classified into magma metal series subclasses by plotting whole rock data from each mine separately on 13 variation diagrams. The field into which samples fell on those variation diagrams determined to which subclass the mine was assigned. After each mining district was classified, variation diagrams that included data from all the mines in each subclass were plotted.

Qualifying the Whole Rock Chemical Analyses

Because representative examples of the six subclasses were needed to define limits and averages, qualifying the data was an important part of this research. The districts were classified based

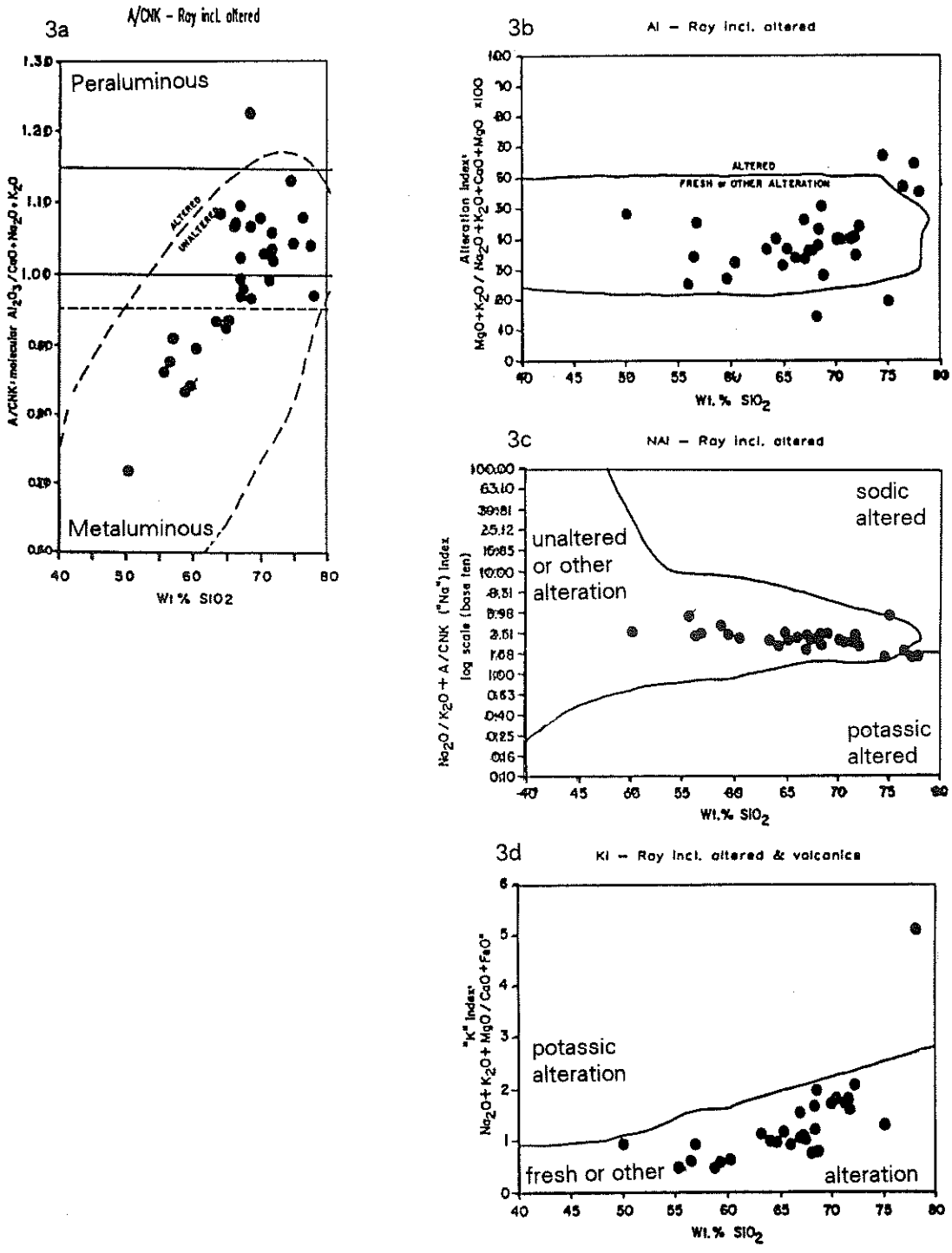

Figure 3. Igneous rocks of the Ray Mining District, Arizona, plotted on magma metal series alteration filter diagrams showing fresh and altered fields. *3a.* Weight percent SiO_2 versus A/CNK, where A/CNK = molecular $Al_2O_3/(CaO + Na_2O + K_2O)$. *3b.* Weight percent SiO_2 versus Alteration Index (AI) = $(MgO + K_2O)/100(Na_2O + K_2O + CaO + MgO)$. *3c.* Weight percent SiO_2 versus sodium index (Na I) = $Na_2O/(K_2O + A/CNK)$ plotted on a log scale (base ten). *3d.* Weight percent SiO_2 versus potassium index (KI) = $(Na_2O + K_2O + MgO)/(CaO + [0.9(Fe_2O_3) + FeO])$.

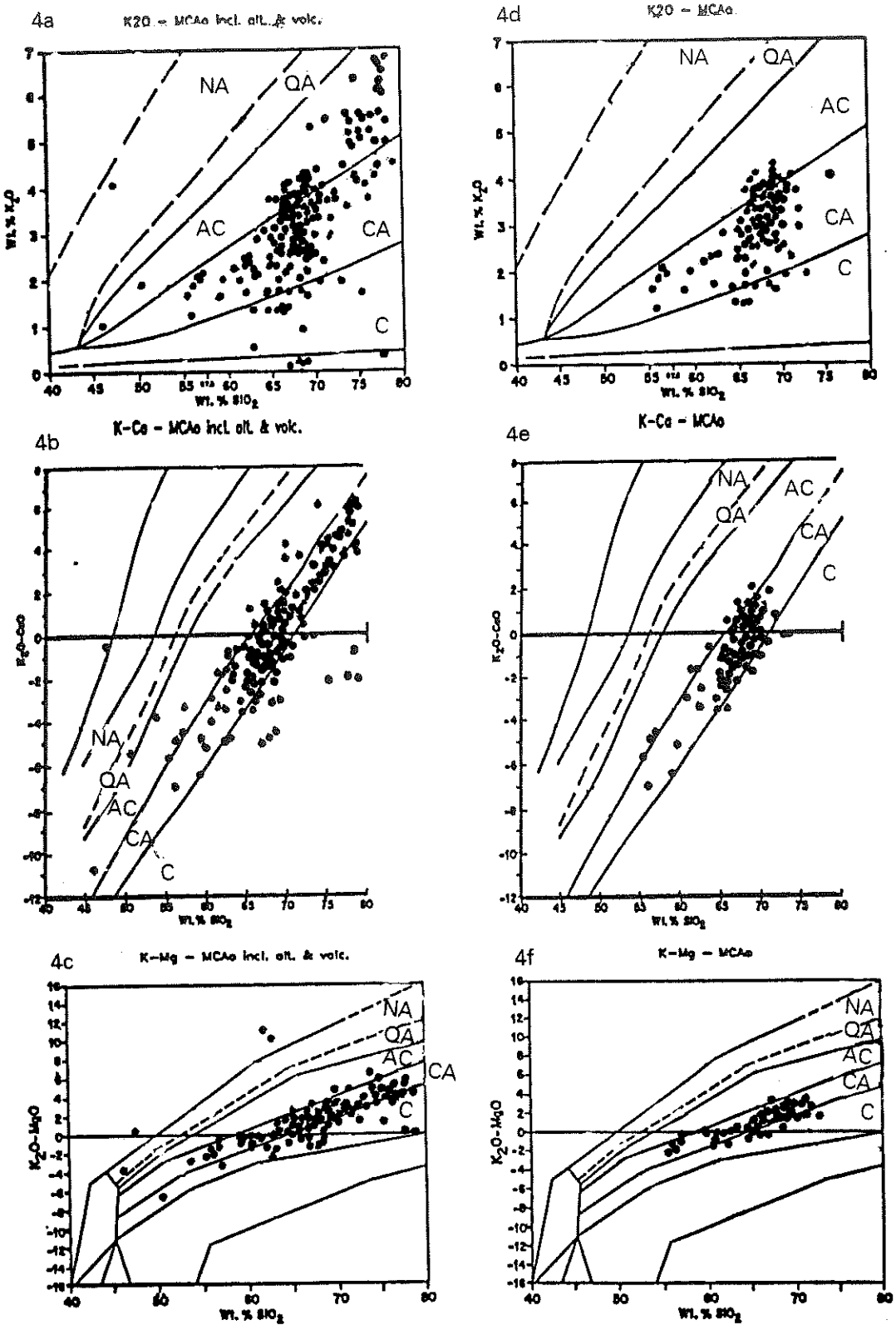

Figure 4. The metaluminous calc-alkalic oxidized class plotted on K_2O versus SiO_2 variation diagram; points scatter outside of field when altered rocks and volcanics are included (on left) and remain within 15 percent of the field using only unaltered rocks (on right). C is calcic, CA is calc-alkalic, AC is alkali-calcic, QA is quartz alkalic, NA is nepheline alkalic.

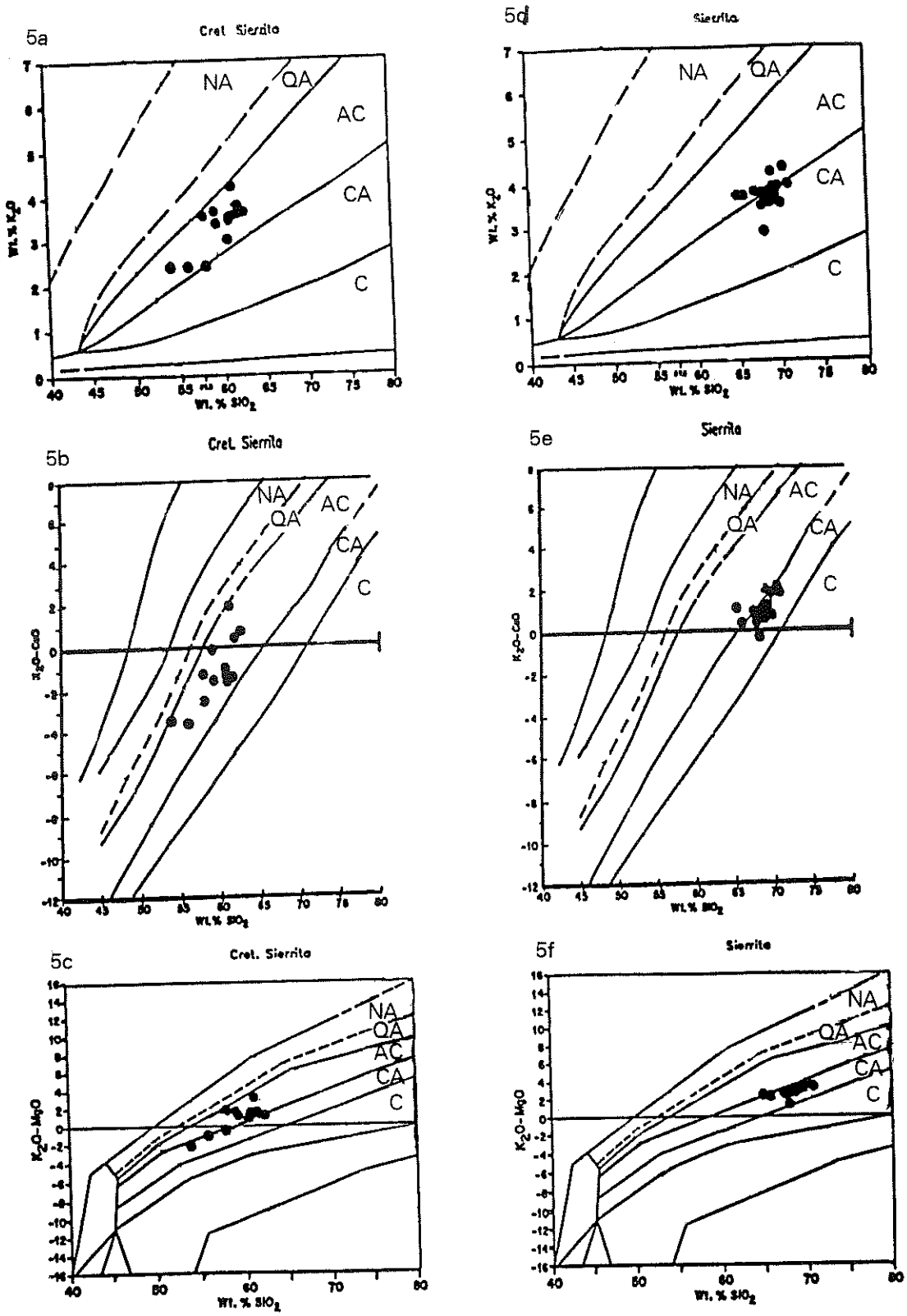

Figure 5. Magma metal series alkalinity graphs of Cretaceous (left side) and Tertiary Ruby Star Granodiorite (right side), in the Pima District, Arizona; NA is nepheline alkalic, QA is quartz alkalic, AC is alkali-calcic, CA is calc-alkalic; C is calcic, M is magnesian.

on plots of unaltered plutonic rocks and on mineralogic criteria. Data from volcanic rocks and samples that did not pass alteration filters were excluded from consideration by discriminant analysis and neural network classification.

Alteration filters (fig. 3) include diagrams with SiO_2 plotted against A/CNK, alteration index, sodium index, potassium index, and loss on ignition. Shand's (1927) A/CNK index is the molecular ratio of Al_2O_3 to total CaO, Na_2O, and K_2O and is calculated by dividing the weight percent of $Al_2O_3/102$ by the sum of the weight percents of CaO/56, $Na_2O/62$, and $K_2O/94$ (fig. 3a). The Alteration index of Ishikawa and others (1976) and Date and others (1983) is calculated by dividing 100 times the sum of K_2O and MgO by the sum of K_2O, MgO, Na_2O, and CaO (fig. 3b). The sodium index is the ratio of Na_2O to the sum of K_2O and A/CNK (fig. 3c). The potassium index is the sum of K_2O, Na_2O, and MgO divided by the sum of CaO, 0.9 Fe_2O_3, and FeO (fig. 3d). Inspection of whole rock chemical data can identify altered plutonic rocks as those with more than 2.5 percent loss on ignition.

The approximate alkalinity of a mining district can be obtained from altered samples, but this practice is risky if there are few sample points or if the samples are severely altered. Comparison of alkalinity diagrams for volcanics and altered rocks with those for unaltered rocks showed a contraction of data into specific fields when altered samples were excluded (fig. 4). Data from twelve of the forty-two districts with whole rock analyses were found to be too altered for reliable classification, so only 30 of the original 90 mining districts were used in the data set for statistical and neural network analysis.

Because altered samples contributed greatly to the scatter on the Fe_2O_3/FeO diagram, the elimination of altered samples from the data base was especially important in determining the oxidation character of the subclasses. Moreover, it was necessary to know the iron mineralogy of igneous rocks and mineral deposits in order to assign a district to an oxidation-reduction subclass particularly for the reduced and weakly oxidized subclasses. In many mining districts the presence of ilmenite in igneous rocks and of pyrrhotite or carbon in mineralized systems indicated reduced status. In other districts the presence of magnetite and sphene in igneous rocks and of pyrite among the primary sulfides indicated oxidized status. Districts with both reduced and oxidized mineralogies were classified as weakly oxidized.

Isotopic age dates and cross-cutting geologic relationships establish links between mineralizing events and particular igneous rocks. It is necessary to determine which phases of a plutonic suite are related to a particular mineralization, which are earlier phases unrelated to mineralization, and which are too altered to be used. In several districts in the western United States magmatism swept eastward during Cretaceous time and back westward during Tertiary time resulting in overprinting of magmatism and mineralization. Magmatism as little as five to ten million years older or younger than an ore deposit can plot in a different alkalinity field, so complex magmatic histories require careful examination to exclude irrelevant rocks. Such care was necessary for Sierrita (fig. 5), Park City, and Tombstone. Because alkalinity changed with time in areas that experienced transgression and regression of subduction-zone magmatism, combining all igneous rocks in a mining district introduces so much scatter on alkalinity plots that correlations between mineralization and whole rock geochemistry of associated plutons are obscured.

Trace Element Geochemistry of Mineralized Samples

If the anions and cations in an ore deposit associated with an igneous complex are the products of differentiation of a cogenetic igneous-metal-volatile suite, then the distribution of metals should be separable into the same subclasses as the igneous suite. Characteristics of mineralized systems can be measured by the quantity and grades of metals produced, types and relative amounts of ore minerals, and concentrations of elements in mineralized rock chip samples.

Statistical Analysis

Standard statistical analysis was used to detect general characteristics of the data, to increase the efficiency of the neural networks, and to classify the samples. Standard petrologic diagrams, magma metal series plots, statistical histograms, and other diagrams were used to characterize the data (Wilt, 1993). Commercial software such as IGPET, RockStat, and SPSS was used to produce comparison diagrams and to categorize subclasses. Discriminant analysis was used to classify analyses of both igneous and mineralized samples into the six magma metal series subclasses of the study.

Neural Network Analysis

Neural networks are a new type of pattern recognition computer software with classification capability. Neural network software excels in pattern recognition, classification, pattern completion, generalization or determination of patterns from examples, and discovery of distinguishing features (Dayhoff, 1990). In contrast with traditional computer software, neural networks are not programmed; they learn from experience, generalize from previous examples, and abstract essential characteristics from input data containing irrelevant information. Most applications use training sets of input data that are paired with their output classes. After each presentation of data in supervised learning, the neural network adjusts the values of its internal weights. If the neural network chooses the right output class for the data that were presented as input, connections are strengthened. If the network chooses incorrectly, connections are weakened and weights are adjusted to minimize error. After enough iterations, the network can produce the correct output class in response to each input pattern.

Neural networks were used in this study to recognize patterns in two sets of data: (1) whole rock analyses of fresh igneous rocks and (2) trace element assays of mineralized rock chip samples from ore deposits associated with those igneous rocks. Mines were grouped according to the magma metal series classification, and neural networks were then trained using geochemical data as input patterns and ore deposit subclasses as output. This procedure was first done with whole rock chemical analyses of igneous rocks as input data and ore deposit subclasses as output. The procedure was then repeated with trace element assays of each sample as input data and ore deposit sub-

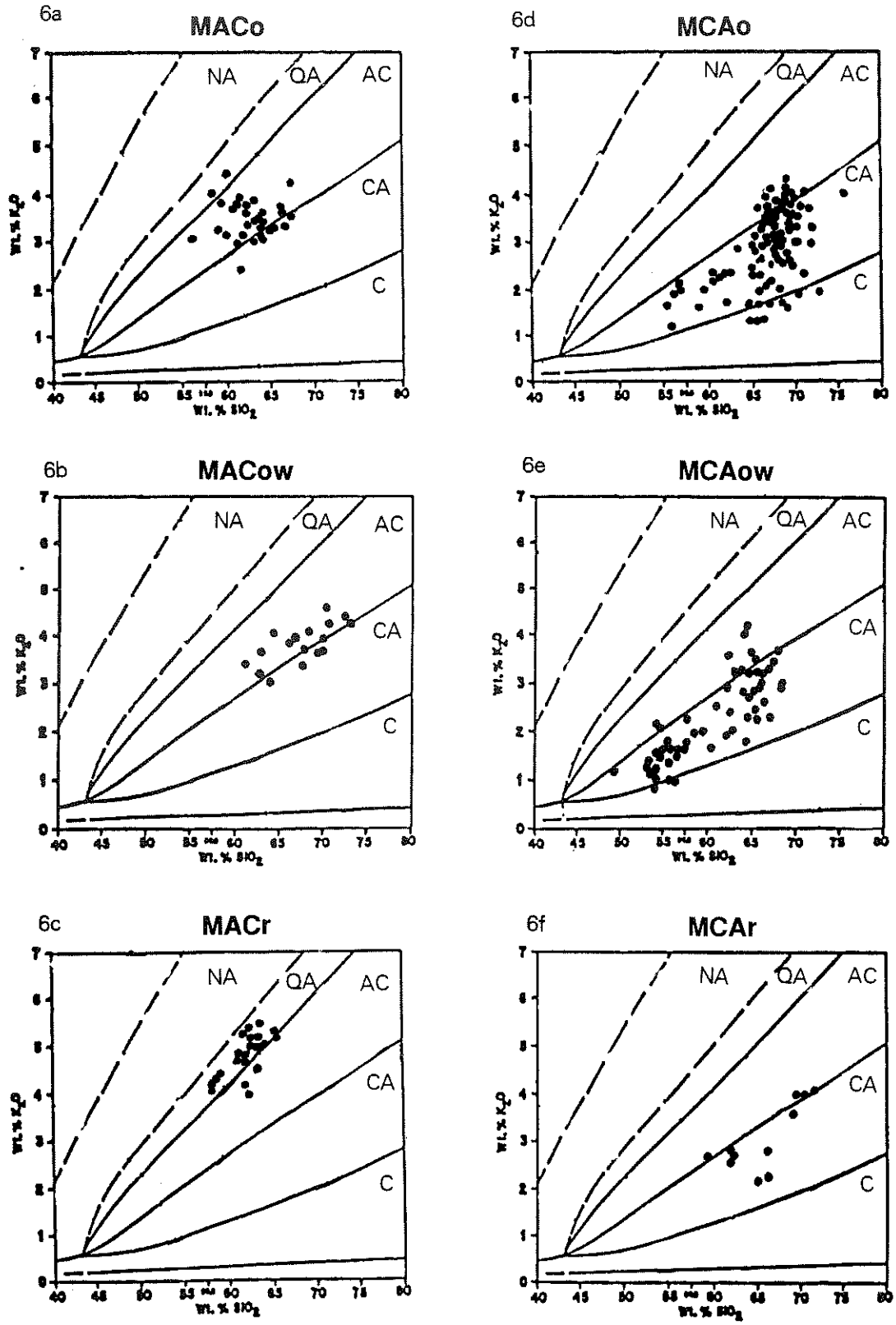

Figure 6. Comparison of K_2O versus SiO_2 variation diagrams for metaluminous alkali-calcic (left side) versus calc-alkalic (right side) and for oxidized (top), weakly oxidized (center), and reduced (bottom) classes. C is calcic, CA is calc-alkalic, AC is alkali-calcic, QA is quartz alkalic, NA is nepheline alkalic.

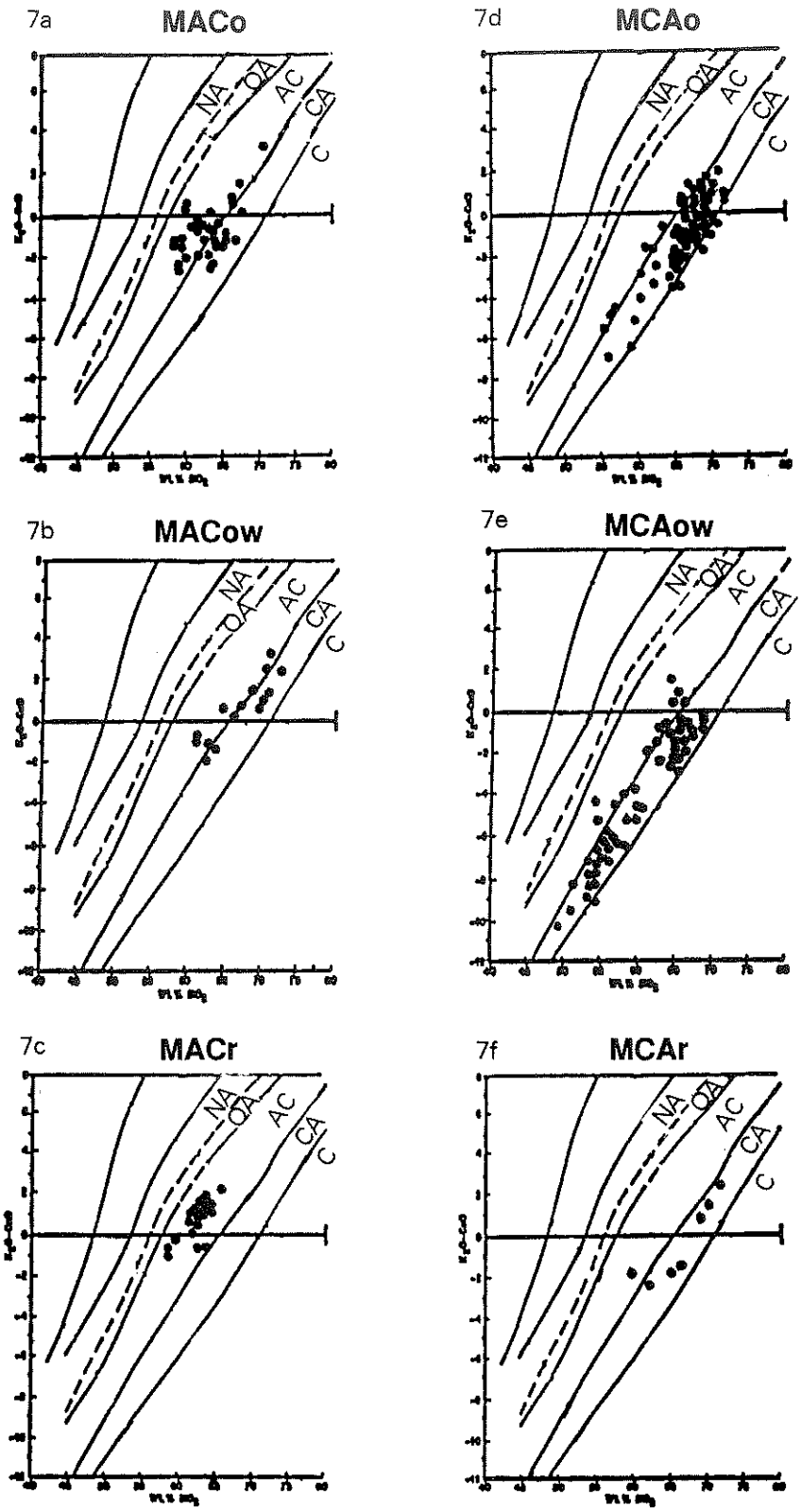

Figure 7. Comparison of K_2O minus CaO versus SiO_2 variation diagrams for metaluminous alkali-calcic (left side) versus calc-alkalic (right side) and for oxidized (top), weakly oxidized (center), and reduced (bottom) classes. C is calcic, CA is calc-alkalic, AC is alkali-calcic, QA is quartz alkalic, NA is nepheline alkalic.

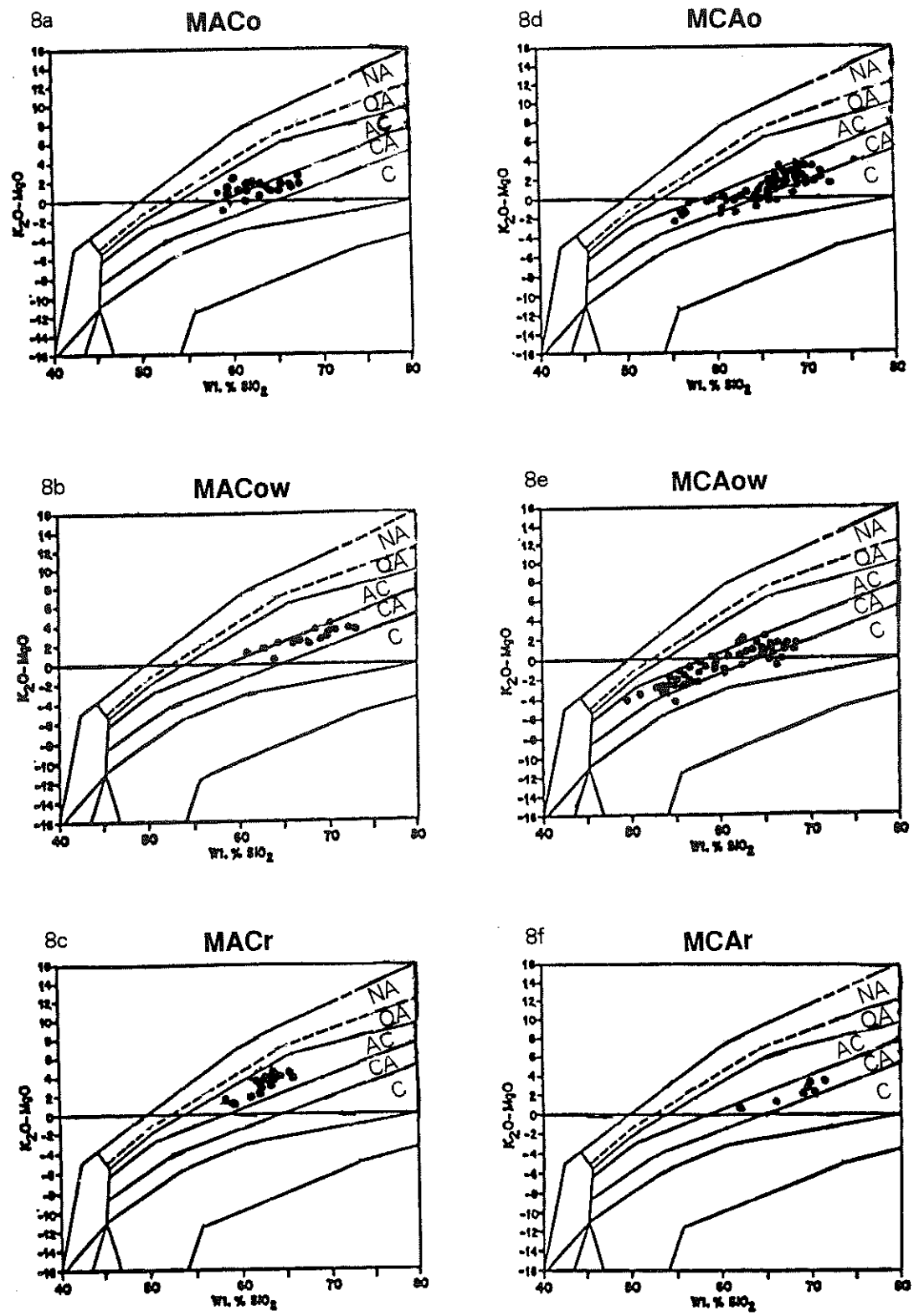

Figure 8. Comparison of K_2O minus MgO versus SiO_2 variation diagrams for metaluminous alkali-calcic (left side) versus calc-alkalic (right side) and for oxidized (top), weakly oxidized (center), and reduced (bottom) classes. C is calcic, CA is calc-alkalic, AC is alkali-calcic, QA is quartz alkalic, NA is nepheline alkalic.

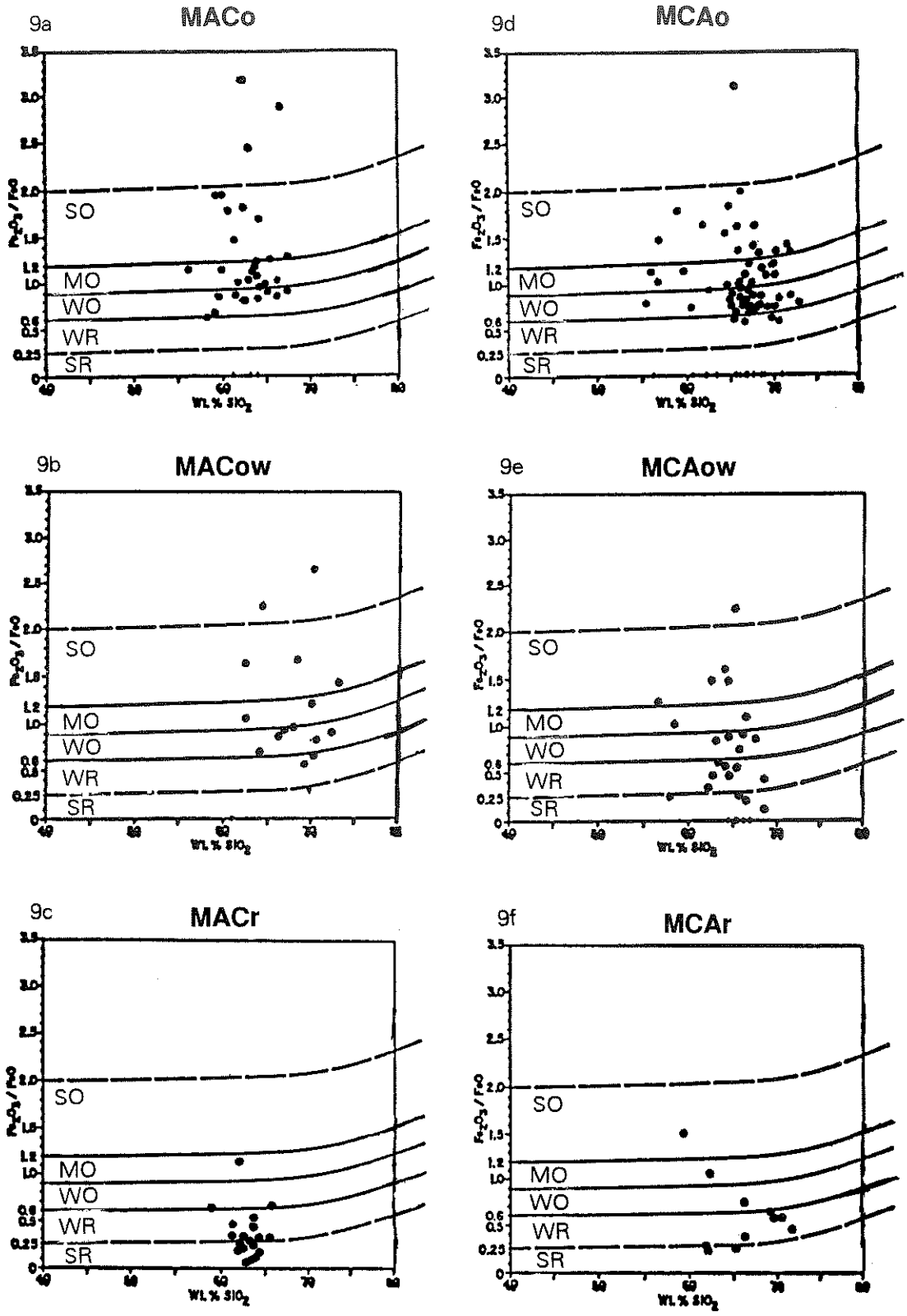

Figure 9. Comparison of Fe_2O_3/FeO versus SiO_2 variation diagrams for metaluminous alkali-calcic (left side) versus calc-alkalic (right side) and for oxidized (top), weakly oxidized (center), and reduced (bottom) subclasses. SO is strongly oxidized, MO is moderately oxidized, WO is weakly oxidized, WR is weakly reduced, and SR is strongly reduced.

Table 2. Characteristic production and mineralogy of six classes studied.

MagmaChem subclasses	Production	Mineralogy
Alkali-calcic oxidized	Pb-Zn-Ag, no Sn Ag-rich Pb, with some Zn, Cu; some dist. Zn prod > Pb; Byproduct Ag and Mn; lesser amts. B, Bi, Ba, Sb, Hg, Au, Be, Te, F;	abund. sulfides (py, cpy, gal, sphal); some enargite; abund. Pb minerals, sulfides, Pb sulfosalts, oxides, sulfates, Pb arsenates, phosphates, Pb vanadates, molybdates; large variety of Ag minerals; Ag sulfides, sulfosalts, halides, Ag tellurides, esp. argentite; Zn carbonates, oxides, sulfates; small amts. Cu minerals; As, Sb, Sn not mentioned; Mn oxides common; native Ag, Au reported
Alkali-calcic weakly oxidized	Pb-Zn-Ag deposits with Sn; also Bi, Mn, B, Hg, As; Ag-rich Pb deposits with byproduct Zn, Cu; similar grades to MACoxidized; but higher Cu+Zn than MACo; have higher Ag:Au ratio;	abund. sulfides (py, cpy, gal, sphal); smaller variety of minerals than MACo; native Ag, Au infrequent; fewer Cu minerals; Cu carbonates reported fewer Pb or Zn minerals; but cerussite, bindheimite, duftite are common; few Ag minerals; argentite, rare sulfosalts and halides are present; no Ag tellurides; Mn oxides, some W, Sb, Fe minerals; no Mo, Bi, As, Sn, Co, Cd, Ni, Tl, Hg or Te min
Alkali-calcic reduced	Sn-Ag deposits; lesser amounts Au,Cu, In, Ga, As, B, Y, F, and P; Ag-rich Sn deposits with no byproduct Au or base metals; very large volume systems	common sulfides (py, cpy, gal, sphal); no mention of native Ag, Au; no Cu, Zn minerals, except tetrahedrite, enargite; anglesite, cerussite reported; not other Pb; lead sulfosalts numerous; huebnerite, wolframite minor; bismuthinite, Sb minerals present; Sn, esp. cassiterite, stannite are common; no Mo, As, Mn, Co, Cd Ni, Tl, Hg, Te minerals;
Calc-alkalic oxidized	major porphyry Cu production; significant Zn & Pb production; Ag prod > Au prod.; some Mo & Mn prod.; lesser amounts of As, B, W; Cu/(Pb+Zn) = 4 to 450 Ag:Au = >40:1 (Ag bias); base:precious = 1000 to 9000:1	abund. common sulfides (py, cpy, gal, sphal, bor); Cu minerals common; abund. molybdenite; common scheelite, rare wolframite; minor native Ag, Au, argentite; no mention of Pb or Zn minerals, Ag halides, Ag sulfosalts, or Ag tellurides; com. mt, hem, lim; arsenopyrite reported; Sb sometimes present; rare bismuthinite; no As, Sn, Co, Cd, Ni, Tl, Hg, or Te

Calc-alkalic weakly oxidized	Au-rich porphyry Cu deposits; byprod. Mo, Zn, Pb, Ag, Au; Cu/(Pb+Zn) 7 to 200,000; Ag:Au = 50:1 to 3:1 (Au bias); base:precious = 200 to 7000:1;	abund. py, cpy, born; minor gal, sphal; scattered native Ag, Au, electrum; common, wide variety Cu minerals; secondary Cu min. abund (az, mal, chrys); cerussite, willemite, smithsonite rare; Ag minerals rare; abund pyrrhotite and arsenopy.; sparse magnetite; com. hematite, marcas.; abund. molbdenite; Bi min. frequent; As & Sb minerals are reported; Mn oxides, Co & Ni minerals occur; no mention of Sn, Cd, Tl, Hg, or Te min.
Calc-alkalic reduced	disseminated Au deposits; generally no byproducts, except some W skarns near plutons; As, Sb, Hg, Tl, W, LREE, Zn, Cu, V, Ni, Ba are characteristic; low sulfur content; no base metal production	abund. pyrite; some cpy, gal, sphal; native Au common; native Ag not present; frequently contain As, Hg, Tl minerals; some secondary Cu minerals, tetrahed.-tennant.; some Pb or Ag sulfosalts; no Zn minerals; some pyrrhotite, rare magnetite; marcasite and arsenopyrite occur in most; molybdenite, scheelite, stibnite common; As min. (realgar, orpiment) gen. present; some Sn and Co min.; Hg (cinnabar) common no Mn, Cd, Ni, Te minerals; wide variety of Tl minerals at Carlin.

Table 2 continued.

classes as output. Ten, twenty, thirty, and fifty percent of the analyses in the geochemical data base were then withheld at random from the data base as a test set and the remaining ninety, eighty, seventy, or fifty percent of the data were used as the training set. Withheld data were then presented to the network for classification, and the resulting output subclasses were evaluated for accuracy.

RESULTS

Whole Rock Subclass Characteristics

Differences among alkalinity subclasses were apparent when all mines from each subclass were plotted on alkalinity variation diagrams. All igneous rocks in the study contained hornblende and were metaluminous, thus samples from all six subclasses plotted in the same general area of the A/CNK diagram. The categorization as alkali-calcic or calc-alkalic was determined on several alkalinity diagrams, but the K_2O against SiO_2 diagram was most reliable (fig. 6). The two subclasses overlapped slightly on the charts, especially where the differentiation index exceeded 85. Alkali-calcic and calc-alkalic rocks were also distinguished on variation diagrams of K_2O – CaO against SiO_2 (fig. 7) and of K_2O – MgO against SiO_2 (fig. 8). There was only minor overlap into adjacent fields among most of the subclasses, but some samples from alkali-calcic oxidized and alkali-calcic weakly oxidized subclasses overlapped into the calc-alkalic field. Degree of oxidation was not reflected in alkalinity diagrams.

All samples in this study were related to mineralized systems, and all were in the moderately iron-poor fields in the FeO^*/MgO versus SiO_2 variation diagram (Wilt, 1993). Exceptions were the relatively barren Cretaceous diorites in the Sierrita district and older barren stocks in the Park City district.

Oxidation subclasses were estimated on a variation diagram of Fe_2O_3/FeO ratio versus silica (fig. 9). All sample points in oxidized subclasses plotted above 0.6 for Fe_2O_3/FeO; some sample points from weakly oxidized subclasses extended into weakly reduced fields between 0.6 and 0.25, and some samples from each mine in the reduced subclasses were below 0.25.

The Fe_2O_3/FeO ratio is sensitive to alteration, weathering, analytical errors, and careless handling; samples can easily become oxidized. Many samples therefore fall into more oxidized portions of the diagram than they would if tested immediately after crystallization. For this reason mineralogic criteria are more reliable in assigning oxidation character. The presence of ilmenite, pyrrhotite, carbon, or graphite suggest reduced or weakly oxidized subclasses while primary magnetite or titanite (sphene) in a plutonic rock or primary pyrite in an ore deposit indicate oxidized subclasses.

Production and Mineralogy of the Subclasses

After mines were assigned to magma metal series subclasses, petrologic, production, and mineralogic information were com-

piled for each mine and grouped to determine metal characteristics of each subclass (Wilt, 1993, appendices). General patterns are summarized in table 2.

Silver:gold ratios of more than 40:1 are a conspicuous characteristic of production from metaluminous alkali-calcic ore deposits. High base-metal contents, high manganese contents, and high lead-zinc ratios are also typical. Alkali-calcic suites are characterized by significant production of silver, lead, zinc, tin, boron, molybdenum, and beryllium; they also have significant byproduct indium, fluorine, lithium, manganese, and tungsten with trace amounts of gold, copper, gallium, iron, uranium, thorium, phosphorus, selenium, mercury, antimony, bromine, arsenic, barium, and magnesium (Keith and others, 1991). Silver production is at least 100 times gold production, and lead and zinc production is ten times copper and molybdenum or tungsten production. Alkali-calcic ore deposits lack molybdenum, cobalt, nickel, thallium, and mercury minerals. Sulfosalts of most metals are present or abundant; tellurides, particularly silver tellurides, are present but rare in oxidized alkali-calcic districts.

Alkali-calcic oxidized districts used in this study include Tombstone, Tintic, Park City, and Castle, Montana. These include vein, skarn, and replacement deposits in which zinc production is greater than lead and silver and manganese are commonly produced as byproducts. Lesser amounts of boron, bismuth, barium, antimony, mercury, gold, beryllium, tellurium and fluorine are also present in these districts.

Alkali-calcic weakly oxidized deposits include the tin-bearing orebodies at Santa Eulalia, Mexico, and Candelaria, Nevada. This type of deposit includes epithermal veins, skarns, and replacements from which lead, zinc, and silver are produced and that have significant associated occurrences of tin, bismuth, manganese, boron, mercury, and arsenic. Districts also include epithermal hotspring deposits that have greater silver production than gold; that include some lead, zinc, and beryllium production; and that have a significant presence of arsenic, antimony, mercury, bismuth, scandium, and fluorine. Alkali-calcic weakly oxidized mining districts used in this study include Taylor, Railroad, Kinsley, Tempiute, Cherry Creek, Linka, and Swales Mountain, Nevada. Alkali-calcic weakly oxidized deposits generally have 100 times less volume than, but similar grades to, alkali-calcic oxidized deposits. Weakly oxidized deposits have higher silver-gold ratios and higher proportions of base to precious metals and of copper and zinc to lead than do deposits of the oxidized subclass.

Alkali-calcic reduced igneous rocks are associated with tin-silver deposits similar to the metaluminous tin-silver deposits of Bolivia. These include epithermal vein, porphyry, skarn, and replacement deposits with tin and silver production and lesser amounts of gold, copper, indium, gallium, arsenic, boron, yttrium, fluorine, and phosphorous. Examples of alkali-calcic reduced mining districts include Llallagua, Oruro, and Potosi, Bolivia. Production from alkali-calcic reduced districts indicates that they are very large volume silver-rich tin deposits with no byproduct gold or base metals. The mining districts of Llallagua, Oruro, and Potosi, Bolivia, each had production of several hundred million kilograms of tin, several tens of millions of kilograms of silver, and no lead, zinc, copper, or gold.

Metaluminous calc-alkalic districts are characterized by significant production of copper, gold, tungsten, and magnesium; by minor production of silver, zinc, lead, molybdenum, antimony, mercury, and sulfur as byproducts; and by significant trace amounts of barium, arsenic, thallium, iron, and selenium (Keith and others, 1991). Production from calc-alkalic ore deposits is dominated by copper over lead and zinc and is relatively silver-poor compared to alkali-calcic districts. Silver production is only ten times higher than gold production, and copper production is 150 times higher than lead and zinc production. Precious metal ratios for oxidized and weakly oxidized subclasses are more silver-rich than for reduced subclasses, which have only gold production.

Calc-alkalic ore deposits generally contain abundant copper minerals, locally important molybdenite and scheelite, and some antimony minerals. Except for galena and sphalerite, lead and zinc minerals are unusual. Antimony, arsenic, cobalt, nickel, thallium, and mercury minerals occur in all calc-alkalic classes and are common in the reduced subclass, but tellurium minerals are lacking.

Calc-alkalic oxidized deposits are similar to the Pima mining district in southern Arizona. These porphyry, skarn, and vein deposits have major production of copper, significant production of zinc and lead, silver production greater than gold production, some molybdenum and manganese production, and trace amounts of arsenic, boron, and tungsten (Keith and others, 1991). Calc-alkalic oxidized districts used in this study include Mineral Park, Red Mountain, Sierrita-Esperanza, Twin Buttes-Mission, Christmas, Ray, Valley Copper and Bethlehem in British Columbia, and Elk Mountain and Mill City in Nevada. The large mining districts, such as Pima, Ray, and Valley Copper and other districts associated with the Guichon Creek batholith have each produced several billion kilograms of copper.

Calc-alkalic weakly oxidized igneous rocks are associated with gold-rich porphyry copper deposits similar to Copper Canyon, Nevada, and Morenci, Arizona. These deposits include porphyry, vein, skarn, and epithermal deposits with significant production of copper, gold, silver, zinc, molybdenum, and lead with lesser amounts of bismuth, arsenic, antimony, vanadium, scandium, and phosphorus (Keith and others, 1991). Calc-alkalic weakly oxidized districts used in this study included Ajo, Dos Pobres, and Morenci, Arizona; Copper Canyon and McCoy, Nevada; El Salvador and El Teniente, Chile; Dexing, China; and Hedley, British Columbia. Some of these mining districts, such as Ajo, Morenci, Copper Canyon, and El Salvador have each produced several billion kilograms of copper.

Calc-alkalic reduced igneous rocks are associated with disseminated gold deposits similar to Carlin-type deposits. These deposits include epithermal, skarn, jasperoid, porphyry, and hot spring deposits that have higher gold production than silver. Lesser amounts of arsenic, antimony, mercury, thallium, tungsten, light rare earth elements, zinc, copper, vanadium, nickel, and barium are also characteristic, as is low sulfur content (Keith and others, 1991). Calc-alkalic reduced districts used in this study include Northumberland, Alligator Ridge, Carlin, Cortez, Chimney Creek North, Maggie Creek, Round Mountain, Getchell, Pinson, and Preble in Nevada and Yellow Pine, Idaho. Some of these mining districts have produced or have reserves of several million kilograms of gold.

Data on production and mineralogy indicated that mineralized systems in this study clustered into groups that correlated with magma metal series igneous classes. Alkali-calcic sub-

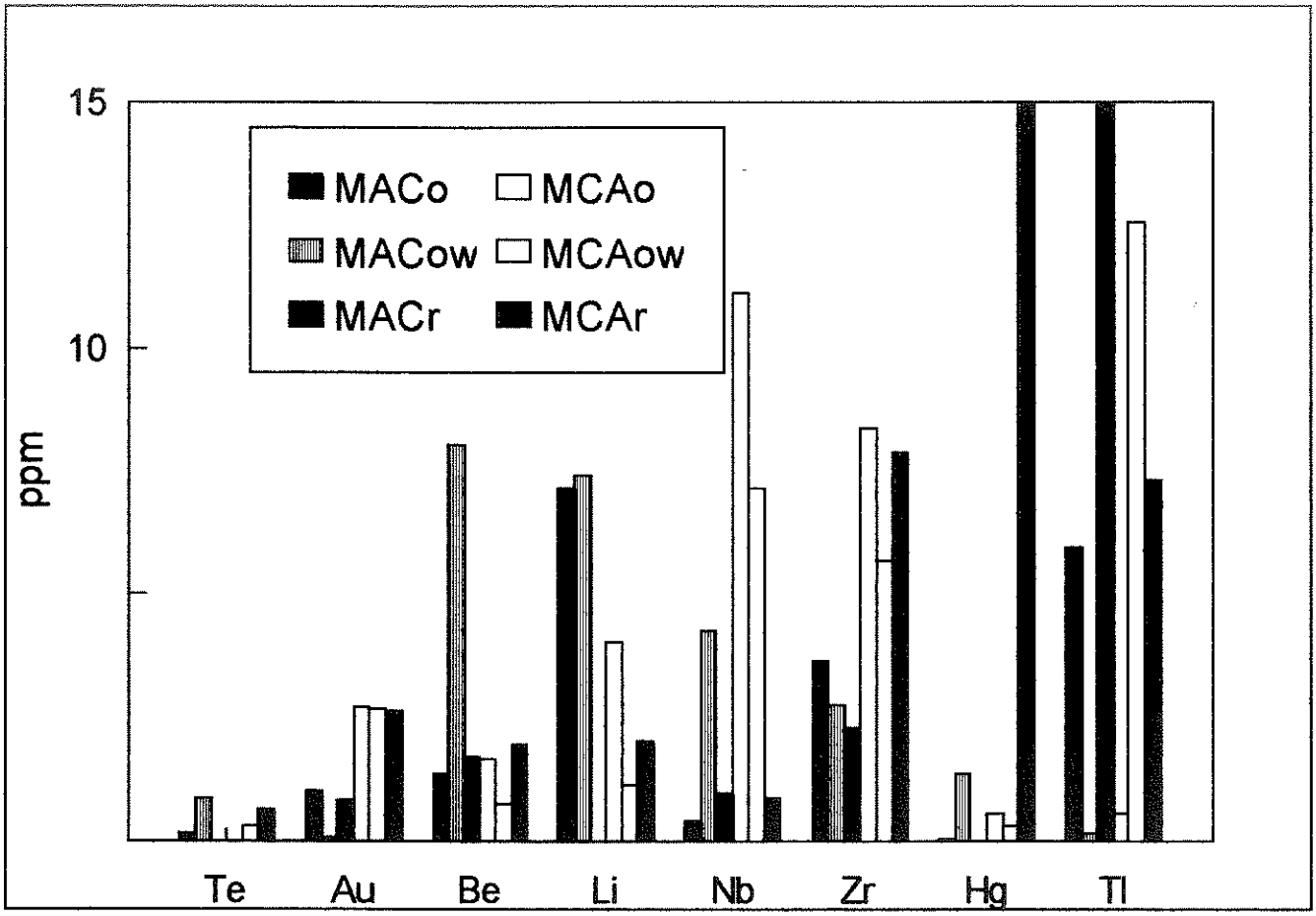

Figure 10. Comparison of means of trace elements from mineralized samples (0 to 15 ppm) showing contrasts among magma metal series classes (MAC = alkali-calcic, MCA = calc-alkalic, o = oxidized, ow = weakly oxidized, r = reduced).

classes had high silver and lead production or grades, whereas calc-alkalic subclasses had high gold or copper production or grades. Oxidized subclasses had high volumes of low grade base metal production and byproduct precious metal production, while reduced subclasses had high volumes of precious metals and low volumes of base metals.

Although mineralogy of various magma metal series subclasses is difficult to quantify, a qualitative tabulation of the data showed clear differences between subclasses (Wilt, 1993). The rich assortment of silver and lead minerals, tin, and manganese in alkali-calcic subclasses and the lack of molybdenum, thallium, and mercury minerals in those subclasses contrasted strongly with the abundant copper minerals, molybdenite, scheelite, and various arsenic, antimony, mercury, and thallium minerals of calc-alkalic subclasses.

Results of Statistical Analysis

Statistical analysis of whole rock oxides indicated a wide variety within each subclass, yet the subclasses were sufficiently different for discriminant analysis to be relatively successful. Means, standard deviations, and variances of whole rock oxides of igneous samples deviated less than did the same statistical parameters of elements of mineralized samples (Wilt, 1993). Because most whole rock oxides varied with silica, their means did not reveal differences among subclasses, but ratios such as SiO_2/K_2O and Fe_2O_3/FeO clearly differentiated the six subclasses.

High variances from the means of each subclass were found for most elements in mineralized rock chip samples, yet many means differed enough to allow the subclasses to be distinguished. For example, alkali-calcic subclasses had 10 to 100 times as much silver as did calc-alkalic subclasses. Most elements did not have a normal distribution; asymmetrical distribution resulted partly from a wide range of data being grouped into 21 equal classes so that most samples fell in the bin closest to zero. The asymmetry also occurred because many samples were not analyzed for all 40 elements and therefore had zero concentrations for some elements.

In spite of the diversity in the data, discriminant analysis was able to properly classify whole rock data for 88 percent of the samples and trace element data for 76 percent of the samples. When mineralized samples were first classified as alkali-calcic or calc-alkalic and then subdivided into oxidation subclasses, discriminant analysis correctly classified 96 percent of alkali-calcic samples and 83 percent of calc-alkalic samples (Wilt, 1993). Despite high variances in the data, the six magma metal series classes were clearly distinguished.

Trace Element Patterns of the Subclasses

Trace element concentrations in parts per million of rock chip samples from mineralized systems had wide variations in their means, standard deviations, and variances. Means of trace elements that varied between 0 and 15 ppm are shown in figure 10, those varying between 20 and 400 are shown in figure 11, and those with concentrations over 1000 ppm are shown in figure 12. General characteristics of element means for each subclass are summarized in table 3, and sample data are in the appendices of Wilt (1993).

Results of Neural Networks Trials

Neural networks accurately classified data from both whole rock and trace element analyses into the same subclasses as those obtained from magma metal series variation diagrams. Results of learning with learning vector quantization were 100 percent accuracy for whole rock oxides and 99 percent accuracy for trace elements from mineralized samples. Results with back propagation were 99.2 percent accuracy for igneous rocks and 93.3 percent accuracy for mineralized samples. Outcomes of testing withheld samples with learning vector quantization ranged from 100 to 85 percent on networks trained on 90 to 50 percent of the whole rock samples, and outcomes of testing withheld samples with back propagation ranged from 100 to 80 percent on networks trained on 90 to 50 percent of the igneous samples. The success of neural networks in classifying the data was encouraging, especially considering the high variability of the data.

Changing the types of data presented to the networks demonstrated the ability of the networks to obtain information about the classes even from ratios and indices derived from whole rock oxides (Wilt, 1993). When the two principal magma metal series classification criteria (SiO_2/K_2O and Fe_2O_3/FeO) were used as the only two input processing elements, the networks performed poorly with less than 60 percent accuracy. However, when additional types of whole rock information were used as input processing elements, the networks were able to correctly classify more cases in less iterations. Neural networks, particularly learning vector quantization, were a very effective means of classifying igneous whole rock data and mineralized trace element data into magma metal series subclasses.

CONCLUSIONS

For a classification to be meaningful and predictive, it must be based on a fundamental truth, organizing principle, or caus-

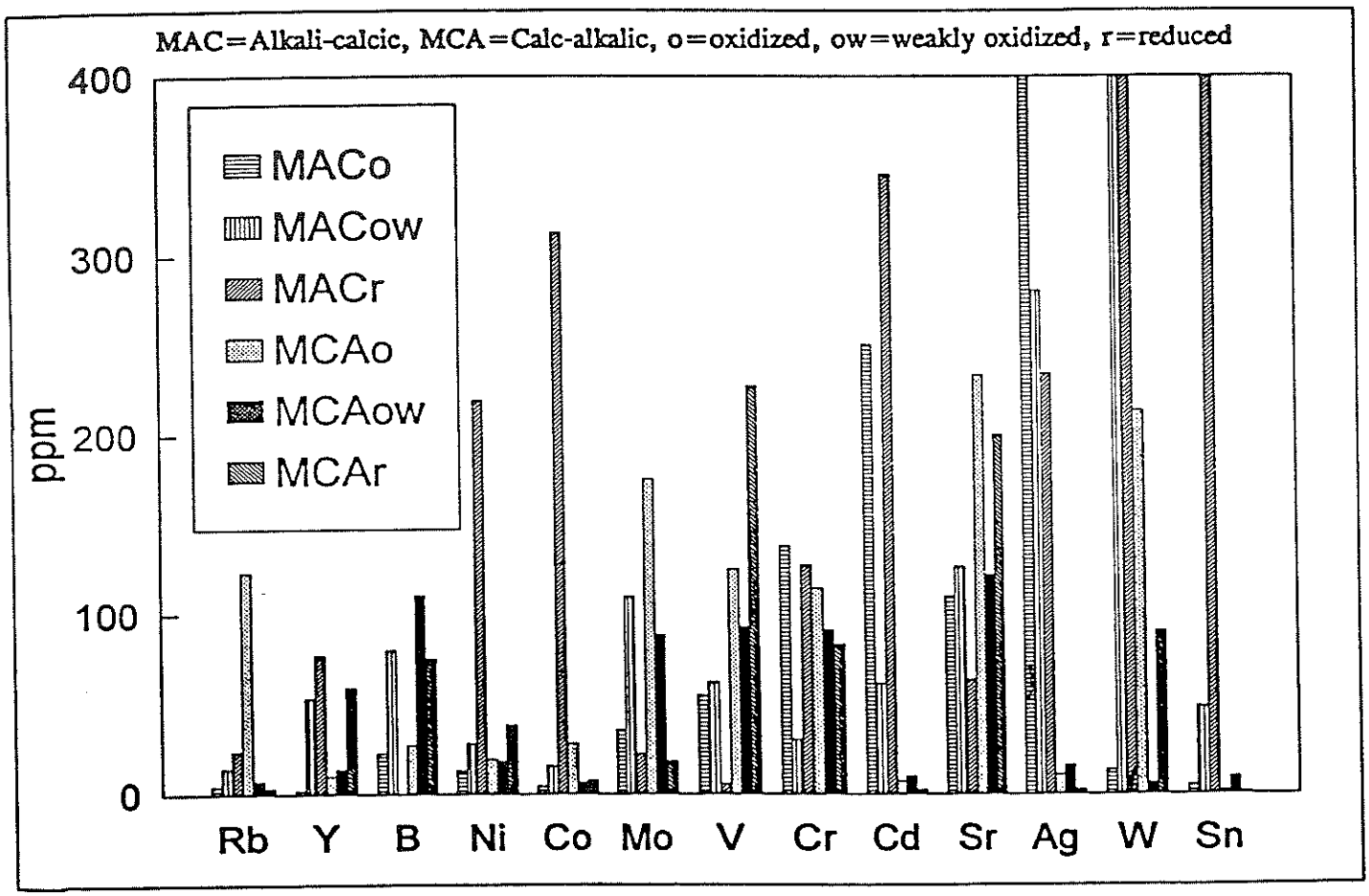

Figure 11. Comparison of means of trace elements from mineralized samples (up to 400 ppm) showing contrasts among magma metal series classes (MAC = alkali-calcic, MCA = calc-alkalic, o = oxidized, ow = weakly oxidized, r = reduced).

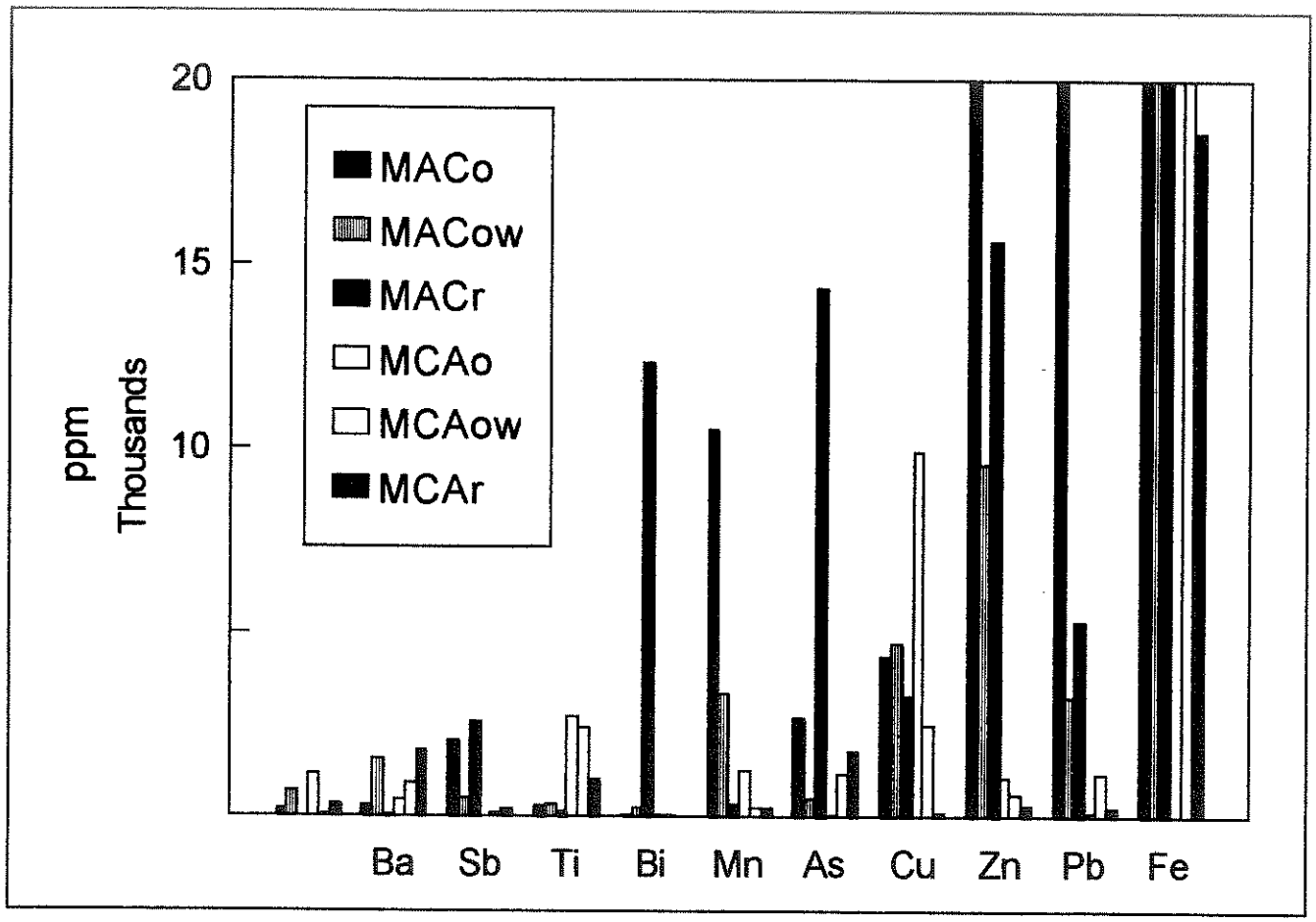

Figure 12. Comparison of means of trace elements from mineralized samples (up to 20,000 ppm) showing contrasts among magma metal series classes (MAC = alkali-calcic, MCA = calc-alkalic, o = oxidized, ow = weakly oxidized, r = reduced).

ative process. Because the magma metal series classification was empirically developed by grouping similar ore deposits together and investigating the geochemistry of fresh igneous rocks related to them, correlation is intrinsic to the classification. If metals in an ore deposit are one of the end products of differentiation of a cogenetic igneous-metal-volatile suite, then ore mineralization should be divisible into the same subclasses as the igneous suites. The high correspondence between chemistries of igneous rocks and related mineralization demonstrated in this study suggests magmatic processes or sources are genetically linked to the ore deposits studied.

The six magma metal series subclasses investigated in this study are internally consistent through all types and scales of chemical information from microscopic trace elements through whole rock oxides and petrology of fresh igneous rocks to ore mineralogy and district-wide metal production. Just as a broken fragment of a holograph transmits the same image as the whole, any type of compositional information can identify the magma metal series subclass.

The excellent results obtained using computer methods are quite remarkable considering the amount of overlap into incorrect fields of some igneous samples and the high degree of variance in mineralized samples. Several samples from each district fell outside of the field occupied by the majority of samples on the variation diagrams, yet neural networks were able to correctly classify even these outlying samples. Neural networks were also able to accurately classify trace element samples in spite of extremely high variances.

Neural networks were very effective in classifying geochemical data into the six magma metal series subclasses examined in this study. When networks that had been trained on 90 to 50 percent of the data were tested with the withheld data, they misclassified less than 20 percent of the test cases regardless of the amount of data withheld. The networks performed best when presented with more kinds of information: The poorest classification success with whole rock samples resulted from using only the two parameters (SiO_2/K_2O and Fe_2O_3/FeO) that were the chief classification criteria in defining the magma metal series subclasses, and the greatest success resulted from using all the whole rock oxides, oxide ratios, some alteration indices, and magnetite and ilmenite concentrations from the modal mineralogy of the plutons. The networks must extract useful classification criteria from oxides and ratios other than the two used to define subclasses in the magma metal series graphical method.

Elem	alkali-calcic ox.	alkali-calcic wkox	alkali-calcic red.	calc-alkalic ox.	calc-alkalic wkox	calc-alkalic red.
Ag	100 - 2,000			<10 - 100		
Au	<6			1 - 40		
As	100 - 4,000	10 - 2,000		10 - 100	100 - 10,000	100 - 10,000
Sb	900 - 5,000	100 - 1,000	100 - 5,000	1 - 40	10 - 800	ave. 100; to 5,000
Hg		0.2 - 30	0.3 - 500	1 - 9	0.2 - 3	
Tl	4 - 50		2 - 400	2 - 7		0.2 - 200
Cu	100 - 6,000	100 - 6,000	10 - 1,000	1,000 - 10,000	1,000 - 10,000	10 - 200
Zn	1,000 - 30,000	100 - 10,000		20 - 200	200 - 1,000	10 - 300
Mn	1,000 - 10,000		100 - 1,000	200 - 2,000	100	100
	10	10	10	100	100	100
Ti	20; to 1,000	100 - 700	10; to 100	1,000	1,000	1,000; to 20,000
Nb				20	20	
Sn	>20	100	1,000; to 30,000	10		
	1 - 20	20; range 1-80		20	20	20
Zr	< 10	< 10	< 10	10; to 100	50	50
Pb	60,000	100; 10 - 10,000	100 - 700	20 - 100	20 - 100	20
Mo	20; < 200	20; to 2,000	20; < 90	20; to 4,000	20; to 10,000	20; to 2,000
	20; 6 - 70	100; 1 - 10,000	100; 8 - 8,000	20; 5 - 5,000	50; 1 - 100	100; 1-7,000
Ba	10 - 100	100; 20 - 10,000	10 - 100	1,000; 100-2,000	1,000; 100-2,000	1,000; 100-2,000
Rb	10; 5 - 50	20; 7 - 1,000	2 - 100	100; 4 - 700	10 - 100	10 - 100
Sr	100; 10 - 700	100; 10 - 700	5 - 60	100; 10 - 700	100; 10 - 700	100; 10 - 700

Table 3. Trace element characteristics of six classes studied (means of samples in parts per million).

Neural networks were much more effective in classifying samples into the six magma metal series subclasses than was discriminant analysis. Neural networks correctly classified 100 percent of the samples; discriminant analysis correctly classified only 76 to 88 percent of the samples. The better performance of neural networks was probably related to the distribution of the data. Most whole rock oxides varied positively or negatively with silica and formed narrow bands on Harker variation diagrams. Because class boundaries were defined by linked changes in two parameters (and particularly the increase in K_2O with increasing SiO_2) no single parameter effectively distinguished between the classes. Even though the whole rock data generally had normal distributions, the means and standard deviations of oxides from different subclasses overlapped.

The poor performance of discriminant analysis on mineralized samples probably resulted from erratic data distribution. Discriminant analysis is based on the assumption that samples have a normal distribution and that different subclasses have distinguishable means and standard deviations and low variances. With an asymmetrical data distribution and missing chemical analyses these assumptions were not fulfilled and means and standard deviations of the mineralized data were not as useful in distinguishing magma metal series subclasses as they are in populations that have normal distributions and complete data sets.

Possible Exploration Applications

Alteration filters used in this study were very effective in eliminating scatter from variation diagrams used to assign mining districts to magma metal series subclasses. Alteration indices, particularly the potassium index, sodium index, A/CNK ratio, and alteration index, would be very effective exploration tools if they were plotted on maps to show areas of a pluton that were most affected by alteration. These spatial alteration patterns could be recognized by neural networks in areas where mineralization is not obvious. Neural networks could also be used to distinguish horizontal or vertical alteration zoning patterns that are characteristic of various ore deposit types or wall rock types.

This study demonstrated the correlation of magma metal series igneous data with six types of ore deposits, and exploration could be based on either kind of information. If mineralization is present, trace element geochemistry of rock chip samples could distinguish what type of ore deposit is potentially present. All examples of each magma metal series subclass do not pro-

duce ore deposits, so standard economic evaluations are also required. However, the assignment of prospects to magma metal series subclasses can indicate if further evaluation is warranted. The magma metal series classification is an inexpensive preliminary step that can eliminate prospects that do not fall into the targeted type of deposit. For example, even though some alkali-calcic oxidized silver deposits have high gold and copper concentrations, they would not make good exploration targets for porphyry copper deposits or Carlin-type gold deposits. If only igneous rocks are present without obvious veins or mineralization, potential mineralization of a particular ore deposit type could be predicted by the magma metal series subclass.

Applications of Neural Networks

The success of neural networks in classifying geochemical data in this study indicates they can be useful in mineral exploration and in deciphering geological systems. Trace element data from exploration projects of unknown ore types can be tested on the networks trained in this study to determine which types of deposits may be found. Once a network is trained on data from either fresh igneous rocks or mineralized trace elements from mining districts of known magma metal series subclasses, the network can be tested on similar types of data from districts whose subclasses are unknown. It is not necessary to obtain whole rock data on fresh igneous rocks related to mineralization in order to correctly assign a mining district to a magma metal series subclass; using neural networks, trace element data from mineralized rock chips can be used to classify the district equally well.

Neural networks can be applied to geologic patterns at many different scales. This study demonstrated patterns in the broadest range of data that could be used to classify types of ore deposits and no attempt was made to distinguish between proximal and distal samples. Within each deposit type, more detailed representations of the areal distribution of the data may allow a neural network to find zoning patterns within trace element data, alteration, fracture density, ore grade or type, or whole rock data. If there are numerically definable differences in the data, neural networks can be trained to detect those differences. The challenge is to define training patterns that have predictive value in exploring for ore deposits. The magma metal series classification has this predictive power because it is empirically based on the correlation between ore deposit types and natural geological processes.

ACKNOWLEDGMENTS

My mother, Jeannette L. Rasmussen, is gratefully acknowledged for financially and emotionally supporting my doctoral studies. Additional financial support was supplied by Grant M. Wilt, by a University of Arizona scholarship established by BHP Minerals, and a grant from the University of Arizona. This study would not have been possible without the generous support in the form of data, ideas, and enthusiastic encouragement from Stanley B. Keith of MagmaChem Exploration, Inc., who supplied thousands of whole rock and trace element chemical analyses which would have cost hundreds of thousands of dollars. These data had been collected during twelve years of consulting for numerous MagmaChem clients and these clients are to be commended for their willingness to share geological data for the advancement of the science.

REFERENCES

Date, J., Watanabe, Y., and Saeki, Y., 1983, Zonal alteration around the Fukazawa Kuroko deposits, Akita Prefecture, Northern Japan: Economic Geology Monograph 5, p. 365-386.

Dayhoff, J., 1990, Neural network architectures, an introduction: New York, Van Nostrand Reinhold, 259 p.

Ishihara, S., 1977, The magnetite-series and ilmenite-series granitic rocks: Mining Geology, v. 27, p. 293-305.

Ishihara, S., 1981, The granitoid series and mineralization: Economic Geology 75th Anniversary Volume, p. 458-484.

Ishikawa, Y., Sawaguchi, T., Iwaya, S., Horiuchi, M., 1976, Delineation of prospecting targets for Kuroko deposits based on modes of volcanism of underlying dacite and alteration haloes: Mining Geology, v. 26, p. 106-117 [in Japanese, with English abstract].

Keith, S.B., 1991, Mid-crustal formation fluids; a solution to the debate on crust vs. mantle as sources of metal for Cordilleran metal deposits: Spokane, Washington, Northwest Mining Association, Left Lateral Leaps, unpublished preprint, 16 p.

Keith, S.B., Laux, D.P., Maughan, J., Schwab, K., Ruff, S., Swan, M.M., Abbott, E., and Friberg, S., 1991, Magma series and metallogeny: a case study from Nevada and environs, *in* Buffa, R.H., and Coyner, A.R., eds., Geology and ore deposits of the Great Basin, Field Trip Guidebook Compendium, vol. 1: Reno, Geological Society of Nevada, p. 404-493.

Miyashiro, A., 1974, Volcanic rock series in island arcs and active continental margins: American Journal of Science, v. 274, p. 321-355.

Peacock, M.A., 1931, Classification of igneous rock series: Journal of Geology, v. 39, p. 54-67.

Shand, S.J., 1927, The eruptive rocks: New York, John Wiley, 488 p.

Takahashi, M., Aramaki, S., and Ishihara, S., 1980, Magnetite-series/ilmenite-series vs. I-type/S-type granitoids: Mining Geology, Special Issue, no. 8, p. 13-28.

Williams, S.A., 1980, The Tombstone District, Cochise County, Arizona: The Mineralogical Record, v. 11, no. 4 (Arizona-II), p. 251-256.

Wilt, J.C., 1993, Geochemical patterns of hydrothermal mineral deposits associated with calc-alkalic and alkali-calcic igneous rocks as evaluated with neural networks: Tucson, University of Arizona, Ph. D. dissertation, 721 p.

Porphyry Copper Deposits of the American Cordillera

Frances Wahl Pierce and John G. Bolm, Editors

Arizona Geological Society Digest 20
1995